Organic & Biomolecular Chemistry

Accepted Manuscript

ROYAL SOCIETY OF CHEMISTRY

www.rsc.org/obc

Surface Patterning with Natural and Synthetic Polymers via an Inverse Electron Demand Diels-Alder Reaction Employing Microcontact Chemistry

Oliver Roling,[a] Artur Mardyukov,[a] Sebastian Lamping,[a] Benjamin Vonhören,[a] Stefan Rinnen,[b] Heinrich F. Arlinghaus,[b] Armido Studer[a] and Bart Jan Ravoo[a,*]

[a] Organisch-Chemisches Institut and Graduate School of Chemistry, Westfälische Wilhelms-Universität Münster, Corrensstraße 40, 48149 Münster, Germany. E-mail: b.j.ravoo@uni-muenster.de; Fax: +49 251 83 36557; Tel: +49 251 83 33287

[b] Physikalisches Institut, Westfälische Wilhelms-Universität Münster, Wilhelm-Klemm-Straße 10, 48149 Münster, Germany.

Abstract

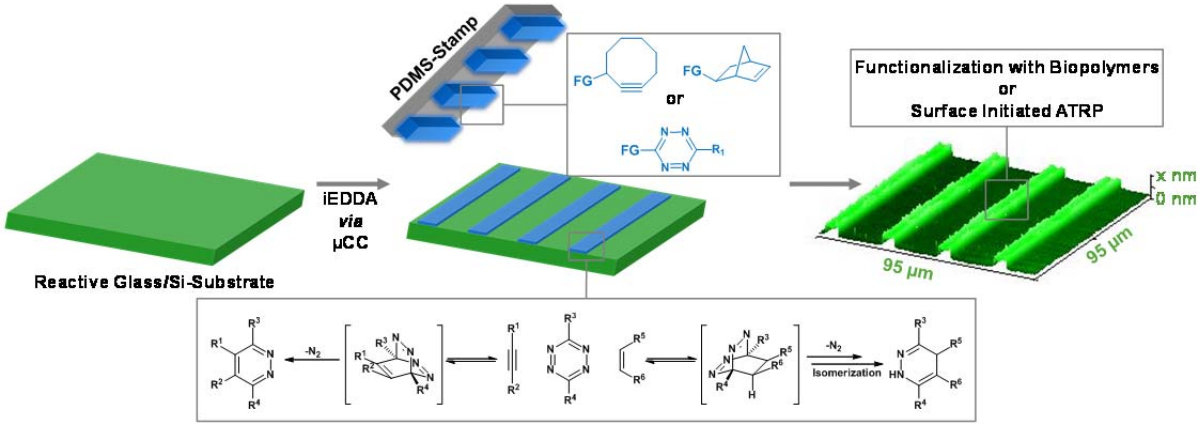

Bioorthogonal ligation methods are the focus of current research due to their versatile applications in biotechnology and materials science for post-functionalization and immobilization of biomolecules. Recently, inverse electron demand Diels-Alder (iEDDA) reactions employing 1,2,4,5-tetrazines as electron deficient dienes emerged as powerful tools in this field. We adapted iEDDA in microcontact chemistry (µCC) in order to create enhanced surface functions. µCC is a straightforward soft-lithography technique which enables fast and large area patterning with high pattern resolutions. In this work, tetrazine functionalized surfaces were reacted with carbohydrates conjugated with norbornene or cyclooctyne acting as strained electron rich dienophiles employing µCC. It was possible to create monofunctional as well as bifunctional substrates which were specifically addressable by proteins. Furthermore we structured glass supported alkene terminated self-assembled monolayers with a tetrazine conjugated atom transfer radical polymerization (ATRP) initiator enabling surface grafted polymerizations of poly(methylacrylate) brushes. The success of the surface initiated iEDDA via µCC as well as the functionalization with natural and synthetic polymers was verified via fluorescence and optical microscopy, X-ray photoelectron spectroscopy (XPS), time-of-flight secondary ion mass spectrometry (ToF-SIMS), atomic force microscopy (AFM) and attenuated total reflection Fourier transform infrared spectroscopy (ATR-FTIR).

Introduction

Structuring metal, glass and semiconductor surfaces with small and large molecules is a key aspect of materials science and nanotechnology due to their potential application in electronic devices or microarrays. Within the last decades a variety of techniques for the patterning of surfaces in the micrometer or submicrometer range emerged. One soft lithography technique with a favourable combination of several advantageous characteristics such as low consumption of material, short patterning times, fast and large area patterning, high pattern resolution, simplicity and high versatility is microcontact printing (μCP).[1] Microcontact chemistry (μCC) is a variation of μCP in which a reactive substrate is brought into close conformal contact with an elastomeric stamp soaked with a molecular ink carrying complementary reactive groups. In μCC a chemical reaction is spatially resolved in the contact area of the substrate and the reactive ink on the stamp. Thus μCC is a straightforward and easy to handle method for the fast functionalization of large areas in a microstructured fashion.[2,3]

A variety of reactions for the functionalization of solid supported reactive self-assembled monolayers (SAMs) has already been reported.[4–9] It was found that especially so-called "click" reactions are very versatile and powerful tools for surface functionalization employing μCC. Among others, thiol-ene and thiol-yne click, Cu(I) catalyzed azide alkyne click, strain promoted azide alkyne click and nitrile oxide click chemistry have been used in order to modify silicon and glass surfaces with different microstructured functionalities.[10–12]

Diels-Alder reactions have been studied intensively as tools for surface ligations as well. In the conventional Diels-Alder reaction, an electron rich diene undergoes a cycloaddition with an electron poor dienophile. Mrksich *et al.* investigated the applicability of the Diels-Alder reaction between cyclopentadiene conjugates and quinones for surface ligations. They conjugated reactive substrates via this approach and were capable of functionalizing a surface bearing quinones with a biotinylated cyclopentadiene.[13,14] Wendeln *et al.* adopted the Diels-Alder reaction in μCC for the fast preparation of simple carbohydrate microarrays. In that work, a variety of carbohydrates were conjugated with dienes and reacted with glass and silicon substrates which were functionalized with SAMs carrying electron poor dienophiles.[15,16] Gevrek *et al.* prepared polymeric coatings on glass with dienes incorporated in the polymer. By doing so they were capable of patterning these substrates via μCC using molecular inks with dienophiles as reactive groups. In this work they were also able to show the reversibility of their surface ligation.[17]

In the inverse electron demand Diels-Alder reaction (iEDDA) an electron deficient diene undergoes a fast reaction with an electron rich double or triple bond without the need for a catalyst or external stimulus. Recently, especially tetrazines have found wide application as electron deficient dienes in the functionalization of polymers, biomolecules, in organic synthesis or for biocompatible applications.[18–30] Independent of the electron rich dienophile, the iEDDA with tetrazine as an electron poor diene starts with a [4+2] cycloaddition. The formed strained bicyclic adducts eliminate nitrogen in rapid retro Diels-Alder reactions. In case of an alkyne, a pyridazine conjugate is obtained, while the reactions with alkenes yield dihydropyridazines. A wide scope of 1,2,4,5-tetrazines with different reactivities and stabilities have already been investigated and many of these substrates undergo fast reactions especially with strained alkenes and alkynes.[31]

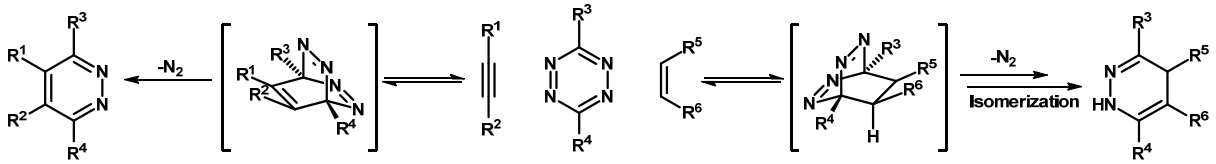

Figure 1: Schematic representation of the reaction between an electron poor 1,2,4,5-tetrazine (middle) and electron rich dieneophiles such as alkynes (left) and alkenes (right).

In 2012 Beckmann et al. presented an elegant approach in which a tetrazine functionalized surface was reacted with carbohydrates carrying a norbornene or terminal alkene as reactive groups employing an automated array printer.[32] In this paper we report surface functionalization utilizing the iEDDA in μCC. By using norbornene or cyclooctyne conjugated carbohydrates, we were capable of modifying glass substrates carrying tetrazines as reactive groups in a microstructured fashion within a few minutes and even seconds. It was not only feasible to prepare monofunctionalized carbohydrate substrates but also orthogonal printing of the reactive dyes was performed (Figure 2a). These bifunctional surfaces were specifically addressable by carbohydrate recognizing proteins belonging to the group of lectins. The successful printing of the dienophiles onto tetrazine functionalized substrates was verified via fluorescence microscopy, X-ray photoelectron spectroscopy (XPS) and time-of-flight secondary ion mass spectrometry (ToF-SIMS).

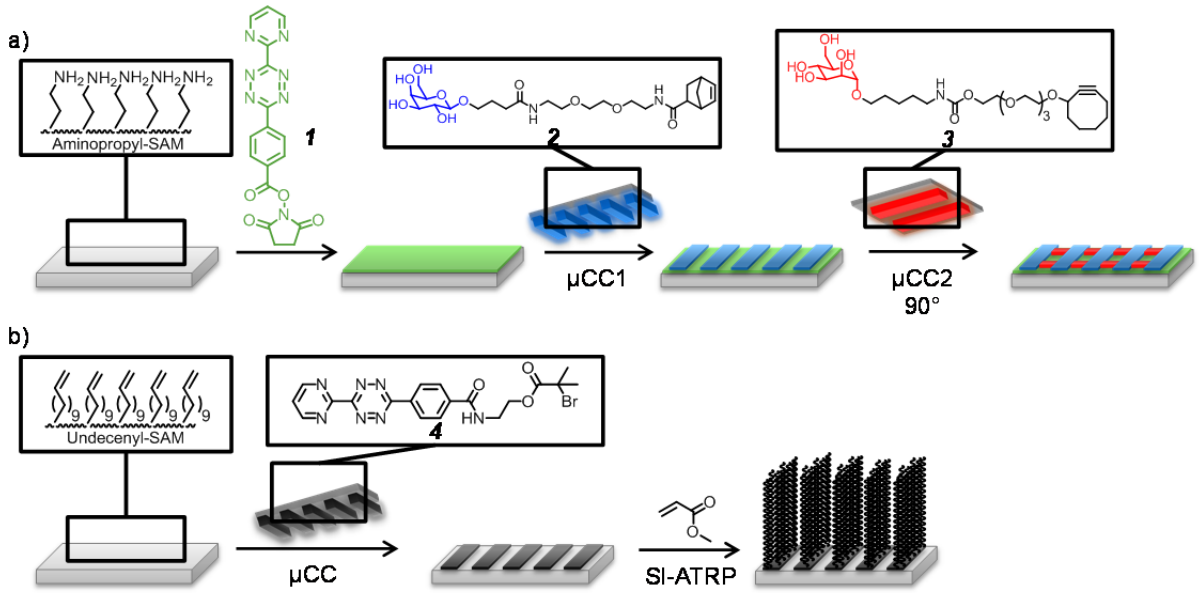

Figure 2: Schematic representation of a) the orthogonal surface modification via inverse electron demand Diels-Alder reaction (iEDDA) and microcontact chemistry (μCC) on a tetrazine functionalized surface and b) the immobilization of the tetrazine conjugated ATRP initiator **4** on a 10-undecenyl trichlorosilane SAM via iEDDA and μCC.

We recently disclosed the applicability of μCC in combination with the radical thiol-ene click reaction for the fast patterning of alkene terminated glass supported SAMs with a nitroxide mediated polymerization initiator. These substrates were used in order to graft various polymer brushes exhibiting versatile supramolecular interactions from the surface.[33] In order to demonstrate the generality of μCC for the preparation of surface grafted polymer brushes, we functionalized alkene terminated SAMs with an atom transfer radical polymerization (ATRP) initiator conjugated with a 1,2,4,5-tetrazine via the combination of μCC and iEDDA. As a proof of principle poly(methylacrylate) (PMA) brushes were grown in a grafting from approach (Figure 2b). The success of the surface initiated polymerization and the patterning of alkene modified substrates via the iEDDA was verified via contact angle goniometry, water condensation experiments, optical microscopy, atomic force microscopy (AFM) and attenuated total reflection Fourier transform infrared spectroscopy (ATR-FTIR).

Results and Discussion

The functionalization of substrates with tetrazine was carried out as reported by Beckmann et al.[32] Aminopropyl triethoxysilane functionalized substrates were immersed into a solution of **1** in a mixture of DMSO and pyridine. Two different carbohydrate conjugated dienophiles are used for the chemical modification of the tetrazine covered substrates. The first one is the

norbornene conjugated galactose derivative **2** and the second one is the mannose tagged cyclooctyne **3** (Figure 2a). Galactose **2** binds selectively to the lectin PNA while mannose **3** binds selectively to the lectin ConA. While **2** was printed onto tetrazine functionalized SAMs using a 25 mM concentration in MeOH with a reaction time of 2 min, the concentration and the printing time for **3** could be reduced. Good pattern resolutions for **3** were obtained at a 10 mM ink concentration in MeOH with a printing time of only 30 s. After printing of the dienophiles, the substrates were washed with ethanol, ultrapure water and sonicated in ethanol for 3 min. As a first proof for the successful immobilization of the respective carbohydrates, fluorescence microscopy imaging with fluorophore tagged PNA and ConA was performed (Figure 3a and b). To this end, the residual tetrazine moieties on the substrates were first blocked by reacting them with neat allylic tetraethylene glycol for 30 min. Subsequently the substrates were blocked with bovine serum albumin (BSA) solubilized in HEPES buffer in order to minimize unspecific binding of the respective lectins. After washing with HEPES buffer, the surfaces were incubated with TRITC labeled ConA and PNA (50 µg/mL in HEPES buffer) for 30 min. This was followed by repeated washing with pure HEPES buffer and fluorescence microscopy imaging.

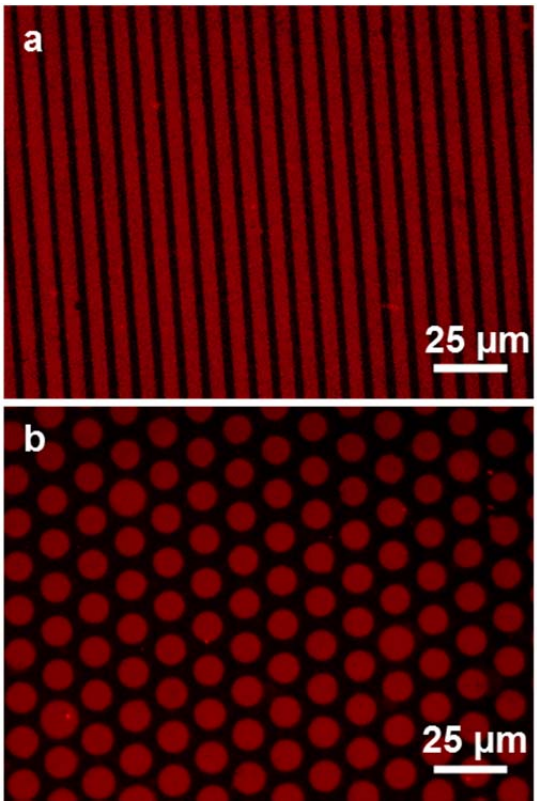

Figure 3: Fluorescence microscopy images of a) galactose **2** printed in 5 µm stripes spaced by 3 µm and incubated with TRITC-PNA (50 µg/mL in HEPES buffer) and b) mannose **3** printed in 10 µm spots spaced by 5 µm and incubated with TRITC-ConA (50 µg/mL in HEPES buffer), both pictures at 40-fold magnification.

Since the printed patterns were successfully visualized via the selective binding of the respective proteins, a first proof for the surface functionalization by the iEDDA employing µCC was given. The selective and homogeneous protein immobilization also confirms a rather high carbohydrate surface density. XPS verified the successful surface initiated iEDDA as well (see Figure S1 in the electronic supporting information, ESI). For this purpose, the fluorinated norbornene **S4** (see ESI for the structure of **S4**) was reacted to a tetrazine functionalized substrate using a flat stamp. Figure S1 shows the N1s signal of a tetrazine functionalized substrate before and after the iEDDA with **S4**. The observed change of the shoulder in the N1s signal (ca 398 eV) may be attributed to the dearomatized structure of the cycloaddition product. The appearance of a fluorine signal (ca 685 eV) in the XPS spectrum results from the immobilized trifluoromethyl group in **S4** and clearly verifies the success of the iEDDA via µCC. Additionally, ToF-SIMS, which is a powerful tool for surface analysis due to its high sensitivity, was carried out. Galactose **2** was printed onto a tetrazine functionalized silicon substrate in 5 µm stripes which were spaced by 15 µm and analyzed by ToF-SIMS. Figure 4 shows an image of the sum of five detected negative ions characteristic for carbohydrates. The observed intensity pattern verifies the successful surface induced iEDDA. This pattern could also be observed on each individual $C_xH_yO_z$ ion, however with less intensity and contrast (see Figure S2 in the ESI).

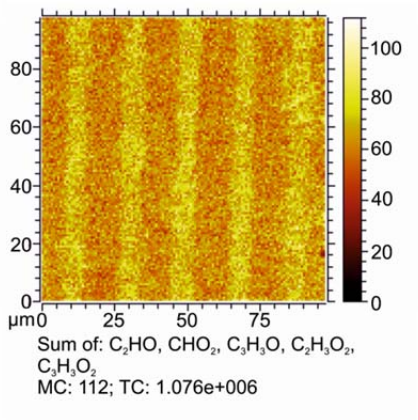

Figure 4: ToF-SIMS analysis of selected negative $C_xH_yO_z$ ions of a tetrazine functionalized silicon surface patterned via µCC with galactose **2** (MC: maximum counts, TC: total counts).

Orthogonal printing of the mannose and galactose conjugates was performed on the same tetrazine surface using the same printing conditions as before. In a first step **2** was printed in 5 µm stripes which were spaced by 15 µm. This was followed by performing an orthogonal printing of **3** in 5 µm stripes which were spaced by 15 µm as well. Finally, the residual tetrazine moieties were saturated with the allylic tetraethylene glycol again. Following the

BSA blocking, these substrates were incubated with FITC-ConA (100 µg/mL in HEPES-buffer) and TRITC-PNA (50 µg/mL in HEPES-buffer). After the incubation with the respective lectin, the substrate was washed with HEPES-buffer, ultrapure water and fluorescence microscopy was performed. Figure 5a shows the orthogonal surface which was incubated with FITC-ConA. The printed stripes are intersected in the expected way since mannose **3** was printed after galactose **2**. The observed intersected stripes also verify the selective protein carbohydrate interaction as no criss cross structure is observed. Subsequently, this orthogonally functionalized substrate was incubated with TRITC-PNA and fluorescence microscopy imaging showed the expected continuous stripes (Figure 5b). The combination of XPS, ToF-SIMS and fluorescence microscopy as well as the orthogonal addressability of bifunctionalized substrates proves the successful surface modification of tetrazine functionalized substrates with carbohydrate conjugated dienophiles via µCC.

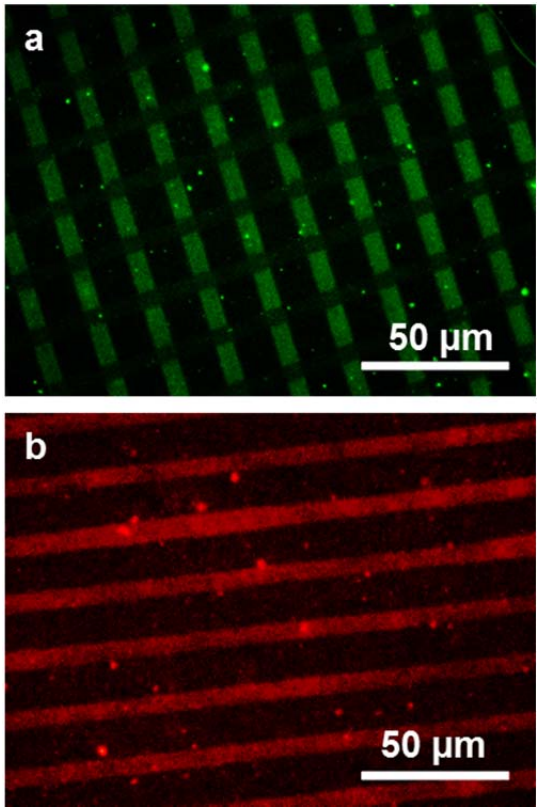

Figure 5: Fluorescence microscopy images of a) intersected stripes caused by mannose **3** printed in 5 µm stripes spaced by 15 µm and incubated with FITC-ConA (100 µg/mL in HEPES buffer) and b) galactose **2** printed before mannose **3** in 5 µm stripes spaced by 15 µm and incubated with TRITC-PNA (50 µg/mL in HEPES buffer), both pictures at 40-fold magnification.

Furthermore we investigated the viability of the iEDDA for the patterning of the tetrazine conjugated ATRP initiator **4** on alkene terminated SAMs and the subsequent surface initiated atom transfer radical polymerization (SI-ATRP). This approach enables a rapid polymer brush functionalization of glass and semiconductor surfaces covered by a reactive SAM. In order to be able to grow polymer brushes in the grafting from approach, a high surface density of polymerization initiators is required. A PDMS stamp patterned with 5 µm stripes spaced by 3 µm was soaked with a 15 mM solution of initiator **4** in methanol which was heated to 60°C. After drying the elastomeric stamp, it was brought into close conformal contact with the alkene functionalized glass substrate. The reaction was allowed to proceed in an oven heated to 60 °C for 55 min. Afterwards the surfaces were washed with ethanol and sonicated in ethanol for 3 min. The success of the iEDDA between the alkene terminated SAM and **4** was verified via contact angle measurements (see Figure S3a-e and Table S1 in the ESI). The water contact angle of the substrate functionalized with **4** decreases compared to the unreacted alkene SAMs. Figure S3d in the ESI shows an alkene terminated SAM on which **4** was printed with a structured stamp. After water condensation onto this substrate, the droplets aligned in the printed structure. Initiator **4** was also printed onto silicon supported alkene SAMs and the printed structures were found in the phase image of the AFM measurements (see Figure S2e in the ESI).

SI-ATRP was conducted by placing an initiator-modified glass under argon atmosphere in a Schlenk tube in an acetone solution containing methyl acrylate, ethyl 2-bromoisobutyrate (EBiB) as a "free" initiator, a 50 ppm $CuBr_2$/tris[2-(dimethylamino)ethyl]amine (Me_6TREN) complex, and ascorbic acid as a reducing agent at 75 °C for 15 h. Figure 6a and b show the AFM image and the corresponding height profile of the resulting PMA brushes. The PMA brushes exhibit a height of around 40 nm and nicely reproduce the printed patterns. Further proof for the successful polymerization is the optical micrograph in Figure 6c as well as the infrared spectrum shown in Figure 6d. The FTIR spectrum exhibits two significant peaks one of which appearing at a wavenumber of 1737 cm^{-1} indicating the methyl ester, while the other at a wavenumber of 1441 cm^{-1} originates from the aliphatic polymer backbone. The collected data emphasize the versatile and fast applicability of the iEDDA employing microcontact chemistry under mild reaction conditions.

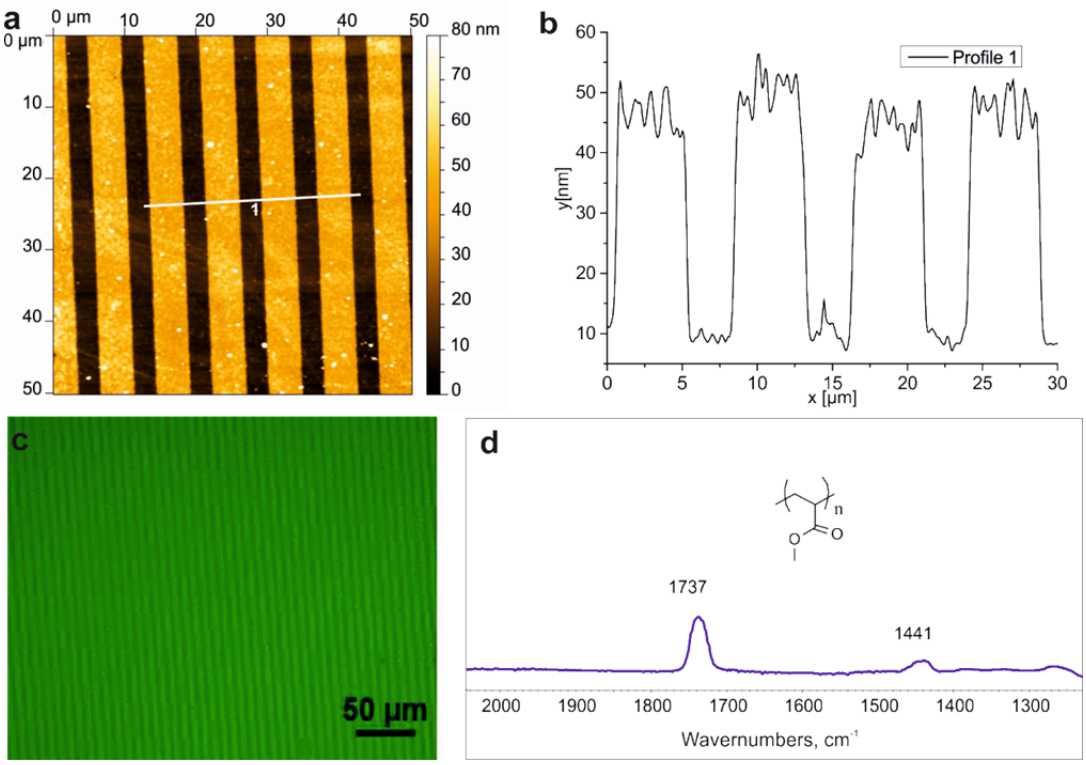

Figure 6: a) AFM image, b) corresponding height profile, c) optical micrograph (20-fold magnification) and d) FTIR spectrum of poly(methyl acrylate) brushes grafted from an alkene terminated glass surfaces patterned with initiator **4**.

Conclusion

In this study we demonstrated the versatility of the iEDDA reaction for chemical surface patterning using µCC. Using iEDDA, it is possible to functionalize tetrazine substrates with dienophiles (and vice versa) at room temperature within a few minutes. The success of the surface induced iEDDA via µCC as well as the following functionalization with natural lectins or synthetic PMA brushes was verified by multiple analytical tools such as contact angle goniometry, XPS, AFM, ToF-SIMS, ATR-FTIR and by light and fluorescence microscopy. These substrates have the potential to be developed to basic biosensors or to structured antifouling coatings. Thus, the iEDDA reaction is a powerful and versatile tool for bioorthogonal surface reactions that can be applied both in biotechnological as well as materials applications.

Experimental Section

General Glass substrates were prepared from IDL microscope slides (Interessengemeinschaft der Laborfachhändler). Detailed information concerning the syntheses of **1**[32], **2** and **3**[11] is available in the literature. The synthesis of **4** and **SI4** is given in the ESI.

Preparation of Aminopropyl SAMs and Functionalization with 1 Glass slides were cut into pieces of approximately 1.4 x 1.4 cm^2 and cleaned by sonication in pentane, acetone and ultrapure water. The substrates were washed with ultrapure water, dried in a stream of argon and subsequently immersed into a freshly prepared piranha solution (conc. H_2SO_4/H_2O_2 (30%); 3/1). After 30 min the substrates were extensively washed with ultrapure water, dried in a stream of argon and put into a freshly prepared solution of aminopropyl triethoxysilane in toluene (2vol.%). After 90 min, the substrates were washed with ethanol, sonicated in ethanol for 3 min and dried in a stream of argon. The surfaces were placed in a flask and the flask was evacuated. The substrates were baked for 10 min at 120 °C. These substrates were immersed into a freshly prepared 5 mM solution of **1** in DMSO/Pyridin (95/5) and stirred for 3 days.[32] Subsequently the substrates were washed with DMSO and acetone and used directly.

Preparation of Undecenyl SAMs Glass slides were cut into pieces of approximately 1.4 x 1.4 cm^2 and cleaned by sonication in pentane, acetone and ultrapure water. The substrates were washed with ultrapure water, dried in a stream of argon and subsequently immersed into a freshly prepared piranha solution (conc. H_2SO_4/H_2O_2 (30%); 3/1). After 30 min the substrates were extensively washed with ultrapure water, dried in a stream of argon and put into a freshly prepared solution of 10-undecenyl trichlorosilane in toluene (0.1vol.%). After 45 min the substrates were taken out of the solution, washed with ethanol and ultrapure water and ready for the μCC procedure after drying the substrates in a stream of argon.

PDMS Stamp Preparation PDMS stamps were prepared by mixing poly(dimethylsiloxane) and curing agent (*Sylgard 184, Dow Corning*) in a 10 to 1 ratio and casting this mixture on a patterned silicon master. The PDMS mixture was cured at 80 °C overnight. Patterned stamps were cut out with a knife and put into a UV ozonizer (*PSD-UV, Novascan Technologies Inc.*) for 55 min prior to use. If not used immediately, the PDMS stamps were stored in distilled water.

μCC Procedure for 2 and 3 Oxidized PDMS stamps were covered with 25 μL of a 25 mM solution of galactose **2** or a 10 mM solution of mannose **3** in methanol respectively. After an

incubation time of 1 min, the stamps were dried in a stream of argon and placed on the tetrazine functionalized substrates. **2** was printed at room temperature for 2 min, while **3** was printed at room temperature for 30 s. Subsequently the substrates were washed with ethanol, ultrapure water and sonicated in ethanol for 3 min.

μCC Procedure for 4 Oxidized PDMS stamps were covered with 25 μL of a 15 mM solution of **4** in methanol which was heated to 60 °C. After an incubation time of approximately 1 min, the stamp was dried in a stream of argon and placed onto the alkene functionalized substrate. The iEDDA was allowed to proceed in an oven at 60 °C for 55 min. Subsequently the surface was washed with ethanol, ultrapure water, DCM and sonicated in DCM for 3 min.

Protein Imobilization Carbohydrate functionalized substrates were covered with a 3 wt% solution of BSA in HEPES buffer (20 mM HEPES, 150 mM NaCl, 1 mM $CaCl_2$, 1 mM $MnCl_2$, pH 7.5) for 30 min and washed with HEPES buffer (2 x 5 min) afterwards. Following the BSA blocking, the substrates were incubated with lectins (either FITC-ConA 100 μg/mL or TRITC-ConA 50 μg/mL plus TRITC-PNA 50 μg/mL in HEPES-buffer) for 30 min. Prior to fluorescence microscopy imaging, the substrates were washed with HEPES-buffer and ultrapure water.

Polymerization Conditions A Schlenk tube was charged with glass slides functionalized with **4** via μCC, methyl acrylate (4.75 g, 55 mmol), ethyl 2-bromoisobutyrate (2.2 mg, 0.0114 mmol), $CuBr_2$ (0.614 mg, 2.75 μmol), and tris[2-(dimethylamino)ethyl]amine (Me_6TREN) ligand in acetone (3 mL). The tube was subjected to three freeze−thaw cycles, then an ascorbic acid (31 mg, 0.175 mmol) was added, and the tube was sealed off under argon. The polymerization was carried out under argon at 75 °C for 15 h. The resulting mixture was cooled to room temperature and dissolved in DCM. The glass was taken out of the solution, rinsed with DCM, followed by ultrasonication (5×) in DCM for 5 min each. The patterned polymer brushes were characterized by AMF, optical microscopy, and ATR-FTIR spectroscopy. DCM was removed from the PMA solution under reduced pressure and the residual monomer was removed in a vacuum-drying cabinet at 60 °C for 12 h. Conversion was evaluated gravimetrically; molecular weight of 280000 g mol^{-1} and polydispersity index (PDI=1.28) were determined by gel permeation chromatography. The brush prepared here shows a high grafting density of 0.96.

X-Ray Photoelectron Spectroscopy XPS measurements were performed with an Axis Ultra DLD (Kratos Analytical Ltd, UK). A monochromatic Al Kα source (*hv* = 1486.6 eV) at

10 mA filament current and 12 kV filament voltage source energies was used. The pass energy was set to 20 eV and the charge neutralizer was used to compensate for sample charging. All measurements were carried out in the "electrostatic mode". The data were evaluated with CasaXPS (version 2.3.15, Casa Software Ltd, UK) and the spectra were calibrated to aliphatic Carbon (C1s = 285 eV)

Time-of-Flight Secondary Ion Mass Spectrometry ToF-SIMS measurements were carried out using a TOF IV compatible instrument equipped with a liquid metal ion gun (IONTOF GmbH, Münster). For analysis 25 keV Bi_3^+ ions were used in a high lateral resolution mode (< 500 nm). A distinct identification of the ions was accomplished by additional analyses, which were performed in a mode with high mass resolution (m/Δm> 7000 at m=41 u) and reduced lateral resolution. The ion images were recorded in an area of 100 x 100 μm^2 with 256 x 256 pixel and a primary ion dose density of 2.57 × 10^{12} cm^{-2}. For data evaluation *Surface Lab 6.3* was used.

Fluorescence Microscopy For fluorescence microscopy imaging an *OLYMPUS CKX 41* microscope was operated with an *OLYMPUS XC 30* camera and a *X-Cite® Series 120Q* by *LUMEN DYNAMICS* as the irradiation source. Data processing was carried out with the software *OLYMPUS Stream Start 1.8*.

Contact Angle Goniometry Water contact angles were measured by means of the sessile drop method on a DSA 100 goniometer (Krüss GmbH Wissenschaftliche Laborgeräte). Contact angle measurements were performed on glass substrates. The evaluation of the measurements was done using the software Drop Shape Analysis, which takes around 100 data points for each measurement and provides a value for the error.

Atomic Force Microscopy For AFM imaging a *NanoWizard 3* from *JPK Instruments* was operated in the tapping mode using *Veeco RTESP-Tapping Mode* etched silicon probes. The AFM was typically operated with a set point of 0.900 V and a scan rate of 1.00 Hz while the AFM images were recorded with 512 x 512 pixels. Data evaluation was done with *gwyddion* (*version 2.22*).

Size exclusion chromatography. SEC was carried out with degased THF or DMF as eluent at a flow rate of 1.0 mL/min at rt on a system consisting of a HPLC Pump 64 (Knauer), a set of two PL gel 5 μm MIXED-C columns (300 × 7.5 mm, Polymer Laboratories) and a Knauer RI differential refractometer detector. Data were analyzed with PSS WinGPC Compact V.7.20 software (Polymer Standards Service) based on calibration curves built upon

poly(methyl methacrylate) standards (Polymer Laboratories Poly(methyl methacrylate) Medium MW Calibration Kit M-M-10 to determine the molecular weight of polymers) with peak molecular weights ranging from 1660 to 1000000 g/mol. The reported GPC data for each individual polymer are the average of several measurements and the GPC profile shown is a representative one.

Fourier transform infrared spectroscopy. FTIR spectra were recorded on a Digilab TFS 4000 equipped with a MKII Golden Gate Single reflection ATR system with diamond crystal 45° top plate P/N 10563. This top plate can be fitted to the Golden Gate optical unit to provide a single reflection 45° specular reflectance measurement of microsamples. The top plate slot aperture is 5 mm × 2.5 mm.

Acknowledgements

The authors thank the Graduate School of Chemistry (fellowship to O. R.) and the Alexander von Humboldt Foundation (postdoctoral fellowship to A. M.). This work was supported by the Deutsche Forschungsgemeinschaft (SFB 858).

Literature

1 Y. Xia and G. M. Whitesides, *Angew. Chem. Int. Ed.* **1998**, *37*, 550–575.

2 C. Wendeln and B. J. Ravoo, *Langmuir* **2012**, *28*, 5527–5538.

3 A. Perl, D. N. Reinhoudt and J. Huskens, *Adv. Mater.* **2009**, *21*, 2257–2268.

4 D. I. Rozkiewicz, W. Brugman, R. M. Kerkhoven, B. J. Ravoo and D. N. Reinhoudt, *J. Am. Chem. Soc.* **2007**, *129*, 11593–11599.

5 A. Calabretta, D. Wasserberg, G. A. Posthuma-Trumpie, V. Subramaniam, A. van Amerongen, R. Corradini, T. Tedeschi, S. Sforza, D. N. Reinhoudt, R. Marchelli, J. Huskens and P. Jonkheijm, *Langmuir* **2011**, *27*, 1536–1542.

6 L. Yan, X.-M. Zhao and G. M. Whitesides, *J. Am. Chem. Soc.* **1998**, *120*, 6179–6180.

7 L. Yan, W. T. S. Huck, X. M. Zhao and G. M. Whitesides, *Langmuir* **1999**, *15*, 1208–1214.

8 C. L. Feng, A. Embrechts, I. Bredebusch, J. Schnekenburger, W. Domschke, G. J. Vancso and H. Schönherr, *Adv. Mater.* **2007**, *19*, 286–290.

9 D. J. Garrett, J. Lehr, G. M. Miskelly and A. J. Downard, *J. Am. Chem. Soc.* **2007**, *129*, 15456–15457.

10 D. I. Rozkiewicz, D. Jańczewski, W. Verboom, B. J. Ravoo and D. N. Reinhoudt, *Angew. Chem. Int. Ed.* **2006**, *45*, 5292–5296.

11 C. Wendeln, I. Singh, S. Rinnen, C. Schulz, H. F. Arlinghaus, G. A. Burley and B. J. Ravoo, *Chem. Sci.* **2012**, *3*, 2479–2484.

12 C. Wendeln, S. Rinnen, C. Schulz, T. Kaufmann, H. F. Arlinghaus and B. J. Ravoo, *Chem. Eur. J.* **2012**, *18*, 5880–5888.

13 M. N. Yousaf and M. Mrksich, *J. Am. Chem. Soc.* **1999**, *121*, 4286–4287.

14 M. N. Yousaf, E. W. L. Chan and M. Mrksich, *Angew. Chem. Int. Ed.* **2000**, *39*, 1943–1946.

15 J. Mehlich and B. J. Ravoo, *Org. Biomol. Chem.* **2011**, *9*, 4108–4115

16 C. Wendeln, A. Heile, H. F. Arlinghaus and B. J. Ravoo, *Langmuir* **2010**, *26*, 4933–4940.

17 T. N. Gevrek, R. N. Ozdeslik, G. S. Sahin, G. Yesilbag, S. Mutlu and A. Sanyal, *Macromol. Chem. Phys.* **2012**, *213*, 166–172.

18 C. F. Hansell, P. Espeel, M. M. Stamenović, I. A. Barker, A. P. Dove, F. E. Du Prez and R. K. O'Reilly, *J. Am. Chem. Soc.* **2011**, *133*, 13828–13831.

19 I. A. Barker, D. J. Hall, C. F. Hansell, F. E. Du Prez, R. K. O'Reilly, A. P. Dove, *Macromol. Rapid Commun.* **2011**, *32*, 1362–1366.

20 H. Stöckmann, A. A. Neves, S. Stairs, K. M. Brindle and F. J. Leeper, *Org. Biomol. Chem.* **2011**, *9*, 7303–7305.

21 M. R. Karver, R. Weissleder and S. A. Hilderbrand, *Bioconjugate Chem.* **2011**, *22*, 2263–2270.

22 M. L. Blackman, M. Royzen and J. M. Fox, *J. Am. Chem. Soc.* **2008**, *130*, 13518–13519.

23 R. A. A. Foster and M. C. Willis, *Chem. Soc. Rev.* **2012**, *42*, 63–76.

24 J. Schoch, M. Wiessler and A. Jäschke, *J. Am. Chem. Soc.* **2010**, *132*, 8846–8847.

25 P. Imming, R. Mohr, E. Müller, W. Overheu and G. Seitz, *Angew. Chem. Int. Ed.* **1982**, *21*, 284–284.

26 M. Wiessler, W. Waldeck, C. Kliem, R. Pipkorn and K. Braun, *Int. J. Med. Sci.* **2010**, *7*, 19–28.

27 N. K. Devaraj, S. Hilderbrand, R. Upadhyay, R. Mazitschek and R. Weissleder, *Angew. Chem. Int. Ed.* **2010**, *49*, 2869–2872.

28 T. Plass, S. Milles, C. Koehler, J. Szymański, R. Mueller, M. Wießler, C. Schultz and E. A. Lemke, *Angew. Chem. Int. Ed.* **2012**, *51*, 4166–4170.

29 C. J. Zhang, C. Y. J. Tan, J. Ge, Z. Na, G. Y. J. Chen, M. Uttamchandani, H. Sun and S. Q. Yao, *Angew. Chem. Int. Ed.* **2013**, *52*, 14060–14064.

30 D. S. Liu, A. Tangpeerachaikul, R. Selvaraj, M. T. Taylor, J. M. Fox and A. Y. Ting, *J. Am. Chem. Soc.* **2012**, *134*, 792–795.

31 A. C. Knall and C. Slugovc, *Chem. Soc. Rev.* **2013**, *42*, 5131–5142.

32 H. S. G. Beckmann, A. Niederwieser, M. Wiessler and V. Wittmann, *Chem. Eur. J.* **2012**, *18*, 6548–6554.

33 O. Roling, A. Mardyukov, J. A. Krings, A. Studer and B. J. Ravoo, *Macromolecules* **2014**, *47*, 2411–2419.